Adsorption Dynamics of Water in Layered Bed for Air-Drying TSA Process

Hyungwoong Ahn and Chang-Ha Lee
Dept. of Chemical Engineering, Yonsei University, Seoul, 120-749, Korea

The thermal swing adsorption (TSA) process is most commonly used to prevent the air contamination from organic solvents of low concentration and to dehumidify gases. Specifically, the air drying by the TSA process is one of the major commercial gas separation processes.

Since the regeneration step in the TSA cycle requires time enough to heat and cool the bed, it is often the time-limiting step in the TSA cycle. In the design and economic assessment of the TSA process, one is principally interested in energy consumption involved with regeneration time, purge gas requirements, and heat load. The equilibrium theory has been widely used to obtain exact solutions from coupled mass and energy balances. In this case, due to the assumption of instantaneous mass- and heat-transfer rates, the predicted concentration and temperature profiles were sharper than the experimental results (Kumar and Dissinger, 1986; Schork and Fair, 1988). However, in the numerical method, the mass and energy balances are solved with the equations describing the mass- and heat-transfer rates. Although this approach has a limit resulting from computational difficulty, it has become a general method to solve the coupled differential equations.

Basmadjian et al. (1975) studied the hot nitrogen regeneration of carbon dioxide in the activated carbon bed by using an adiabatic model. Carter and Husain (1974) have carried out both experiment and simulation of the adsorption breakthrough of carbon dioxide and water with helium as a carrier gas in a fixed bed. They found that a surface or capillary flow of adsorbate occurs in the adsorbed phase transport in addition to macropore diffusion. Also, the adsorption and desorption of ethane and propane mixtures on activated carbon by using a nonisothermal model with Flory-Huggins solution theory (FH-VSM) and a rate model considering Knudsen and surface diffusions in parallel (Huang and Fair, 1988). Davis and LeVan (1987) showed that adiabatic fixed-bed adsorption cycles with adsorption, heating, and cooling steps were analyzed by using simple wave theory.

Although the air-drying TSA process is commonly used in industry, there has been little fundamental research to improve an understanding of the process. Moreover, an extensive literature on adsorber analysis has been published, but relatively few theoretical analyses have been done on regeneration (Yang, 1987; Ruthven et al., 1994). However, it is usually the regeneration step that determines the economic success of the TSA process, because it consumes a huge amount of energy for regeneration. Therefore, the improvement of the regeneration process through the minimization of energy consumption can contribute to the design and optimization methods of the TSA process. In addition, Yang and Lee (1998) studied the adsorption dynamics of a layered bed for the purpose of developing a H_2 PSA process from coke oven gas. The performance of the PSA process could be improved by using the layered bed packed with both activated carbon and zeolite 5A in comparison to the single adsorbent bed. Recently, the prepurification of air including water was studied by the PSA process, with single and layered beds using zeolite 13X as one of the commercial adsorbents (Rege et al., 2001). However, while PSA processes using a layered bed have been widely studied (Park et al., 1998; Watson et al., 1996; Lee et al., 1999; Ahn et al., 1999), it is hardly studied for the TSA process with a layered bed.

In the engineering plastic industry and pharmaceutical industry, a small-scale air-drying TSA process with zeolite is widely used to produce dry air with an extremely low dew point. The purpose of this study is to understand the adsorption dynamic of the air-drying TSA process. While it was well known that silica gel was suitable for the bulk separation of water, the zeolite was superior to silica gel for the treatment of humid gas with a very low dew point. In this study, the dynamics of water adsorption and thermal regeneration in the zeolite 13X bed was compared with that in the layered bed with zeolite 13X and silica gel. Based on the breakthrough and regeneration dynamics, the two-bed, two-step TSA process was simulated in both the zeolite 13X bed and the layered bed.

Mathematical Model

Because the adsorption capacity of water in zeolite 13X was incomparably greater than that of nitrogen as a carrier

Correspondence concerning this article should be addressed to C.-H. Lee.

gas, the contribution of nitrogen to the total adsorption dynamics could be negligible. Therefore, this binary component system can be simplified to a single-component system for water vapor. The assumptions in the model are as follows: (1) the flow pattern can be described by an axially dispersed plug-flow model; (2) the gas phase behaves as an ideal gas mixture; (3) the solid and gas phases reach thermal equilibrium instantaneously; (4) axial conduction in the column wall can be neglected; (5) radial concentration and temperature gradients in the adsorption bed are negligible; and (6) pressure drop along the bed is neglected. These assumptions were widely accepted by several studies in the adsorption process (Yang, 1987; Hwang et al., 1997; Yang and Lee, 1998). Also, Farooq and Ruthven (1990) pointed out that the radial effect of temperature becomes negligible as the system approaches the adiabatic behavior.

To understand the dynamics of water adsorption and thermal regeneration, the nonisothermal and nonadiabatic model from previous studies (Lee et al., 1999; Yang and Lee, 1998) was used and the model was transformed to the dimensionless form in this study.

The single-component mass balance through a packed bed was as follows

$$\frac{\partial y}{\partial \tau} - \frac{1}{Pe_m}\frac{\partial^2 y}{\partial \zeta^2} + \frac{\partial yU}{\partial \zeta} + A\frac{\partial \overline{Q}}{\partial \tau} = 0. \tag{1}$$

Neglecting the pressure variation along the bed, including the pressure drop, the overall mass balance was as follows

$$\frac{\partial U}{\partial \zeta} - \frac{1}{\Theta}\frac{\partial \Theta}{\partial \tau} - \frac{U}{\Theta}\frac{\partial \Theta}{\partial \zeta} + A'\Theta\frac{\partial \overline{Q}}{\partial \tau} = 0. \tag{2}$$

The depth of the temperature variation in the TSA process has a great effect on the total process. Therefore, the energy balance in the gas and solid phases with the heat transfer to the column wall was constructed as follows:

$$-\frac{1}{Pe_h}\frac{\partial^2 \Theta}{\partial \zeta^2} + \frac{\partial \Theta}{\partial \tau} + BU\frac{\partial \Theta}{\partial \zeta} - C\frac{\partial \overline{Q}}{\partial \tau} + D(\Theta - \Theta_w) = 0. \tag{3}$$

The heat capacity of the adsorbed phase was considered in Eq. 3 because of the large heat capacity of water. Liu and Ritter (1997) suggested a cubic temperature dependence for the prediction of the heat capacity of gas in simulating the PSA process for the solvent vapor recovery. The same cubic equation was used in this study and all the parameters in the cubic equation came from Reid et al. (1988).

In this study, heat loss through the column wall and heat accumulation in the wall were considered because the temperature change in the wrapped glass wool during the regeneration experiment was monitored. Therefore, another energy balance in the column wall was used as follows

$$\frac{\partial \Theta_w}{\partial \tau} - E(\Theta - \Theta_w) + F\left(\Theta_w - \Theta|_{T_{atm}}\right) = 0. \tag{4}$$

The effect of heat transfer at the wall is very important in the TSA process in comparison to the PSA process, due to the flow of hot purge gas in the regeneration step. The separate experiments were performed in order to estimate the heat-transfer coefficient at the wall. The adsorption bed was packed with the clean zeolite 13X pellet, and then the bed was heated by a hot nitrogen purge at various temperatures and flow rates. The inner and outer heat-transfer coefficients at the wall were determined by matching the energy balance to the experimental data both in the bed and in the wall (Hwang et al., 1997; Ahn, 2002).

In this study, the Langmuir–Freundlich (L-F) isotherm model and linear driving force (LDF) model were used for adsorption equilibrium and rate, respectively

$$Q^* = \frac{Q_m(y\Theta G)^n}{1+(y\Theta G)^n} \tag{5}$$

$$\frac{\partial \overline{Q}}{\partial \tau} = H(Q^* - \overline{Q}). \tag{6}$$

The LDF coefficients for adsorption and regeneration in both the zeolite 13X and the silica gel are presented in Table 1.

The boundary condition for the adsorption breakthrough could be written by

$$y(\tau,0) = 1, \qquad \Theta(\tau,0) = 1 \tag{7a}$$

$$\left.\frac{\partial y}{\partial \zeta}\right|_{\zeta=1} = 0, \qquad \left.\frac{\partial \Theta}{\partial \zeta}\right|_{\zeta=1} = 0. \tag{7b}$$

A "clean bed" condition was used as the associated initial condition for the adsorption breakthrough

$$y(0,\zeta) = 0, \qquad \Theta(0,\zeta) = \Theta Q|_{T_{atm}}. \tag{8}$$

Table 1. Characteristics of Adsorption Bed

Bed length	30.0 cm	
Inner bed diameter	3.3 cm	
Flange length	4.0 cm	
Flange diameter	6.3 cm	
Column thickness	0.23 cm	
Column density	7.83 g/cm^3	
Heat capacity of column	0.50 J/g·K	
Inner heat transfer coefficient (at 473 K, 26 LSTP/min)	4.2×10^{-3} J/cm^2·s·K	
Outer heat transfer coefficient	4.2×10^{-4} J/cm^2·s·K	
	Zeolite 13X	Silica Gel
Bed void fraction	0.37	0.26
Total void fraction	0.52	0.47
Bed density	0.69 g/cm^3	0.82 g/cm^3
Overall mass transfer coefficient for adsorption (at 9 LSTP/min)	7.5×10^{-4} s^{-1}	4.5×10^{-4} s^{-1}
Overall mass transfer coefficient for regeneration (at 26 LSTP/min)	0.075 s^{-1}	0.075 s^{-1}

The boundary condition for the regeneration breakthrough was as follows

$$\left.\frac{\partial y}{\partial \zeta}\right|_{\zeta=0}=0, \qquad \left.\frac{\partial \Theta}{\partial \zeta}\right|_{\zeta=0}=0 \tag{9a}$$

$$y(\tau,1)=0, \qquad \Theta(\tau,1)=1. \tag{9b}$$

A "saturated bed" condition was used as the initial condition for the regeneration breakthrough together with the condition of the uniformly adsorbed phase

$$y(0,\zeta)=1, \qquad \Theta(0,\zeta)=\Theta|_{T_{\text{atm}}}. \tag{10}$$

The following dimensionless variables and parameters were used in expressing the preceding dimensionless equations:

$$\tau=\frac{u_0 t}{L}, \qquad \zeta=\frac{z}{L}, \qquad y=\frac{c_i}{c_0}, \qquad \bar{Q}=\frac{\bar{q}}{q_0},$$

$$Q^*=\frac{q^*}{q_0}, \qquad Q_m=\frac{q_m}{q_0}, \qquad \Theta=\frac{T}{T_f}, \qquad \Theta_w=\frac{T_w}{T_f},$$

$$U=\frac{u}{u_0} \tag{11a}$$

$$Pe_m=\frac{u_0 L}{D_L}, \qquad Pe_h=\frac{u_0 L\beta}{K_L},$$

$$A=\frac{(1-\epsilon)\rho_P q_0}{\epsilon c_0}=\frac{(1-\epsilon)RT_f\rho_P q_0}{\epsilon P_i},$$

$$A'=\frac{(1-\epsilon)RT_f\rho_P q_0}{\epsilon P_{\text{tot}}}$$

$$B=\frac{\epsilon\rho_g C_{Pg}}{\beta}, \qquad C=\frac{\rho_B \triangle H q_0}{\beta T_f}, \qquad D=\frac{2h_i L}{R_{Bi}u_0\beta},$$

$$E=\frac{2\pi R_{Bi}h_i L}{\rho_w C_{Pw}A_w u_0}, \qquad F=\frac{2\pi R_{Bo}h_o L}{\rho_w C_{Pw}A_w u_0},$$

$$G=b^{1/n}P_f, \qquad H=\frac{kL}{u_0}, \tag{11b}$$

where

$$\beta=\alpha\rho_g C_{Pg}+\rho_B C_{Ps}+\rho_B\bar{Q}q_0 C_{Pa}M_a.$$

In this study, an adsorption bed with a large flange was used. The flange of the adsorption bed can work as a heat sink in the adsorption and regeneration breakthroughs. Therefore, the temperature of a hot fluid in the bed might be slightly lower than expected. Since the flange effect is similar to the heat transfer by extended surface equipment, it is expressed by an additional boundary condition for the adsorption step as follows

$$\left.\frac{R_{Bo}}{A_w}\right|_{\zeta=1}=\frac{\pi R_F+\pi\eta\left(R_F^2-R_{Bi}^2\right)}{\pi t_F\left(R_F^2-R_{Bi}^2\right)}. \tag{12a}$$

And the corresponding boundary condition for the regeneration step is

$$\left.\frac{R_{Bo}}{A_w}\right|_{\zeta=0}=\frac{\pi R_F+\pi\eta\left(R_F^2-R_{Bi}^2\right)}{\pi t_F\left(R_F^2-R_{Bi}^2\right)}. \tag{12b}$$

In Eq. 12, the fin efficiency, η, was estimated to be 0.5.

In this study, the dimensionless PDEs for mass and energy balance with proper initial and boundary conditions were reduced to a set of ordinary differential equations (ODEs) by a method of lines. First-order downward difference scheme and second-order central difference scheme were used to approximate the first-order and second-order spatial derivatives, respectively. This numerical method is able to resolve first-order temporal and second-order spatial hyperbolic partial differential equations with a substantial reduction in numerical oscillation and diffusion. Then, the final set of ODEs was solved by using the DASSL.

Experiment

Water used in the feed mixture was produced in an ultrapure system (Barnstead, D4641). Nitrogen was used as a carrier gas in the adsorption breakthrough and as a hot purge gas in the regeneration breakthrough. The zeolite 13X (Aldrich Co.) and the silica gel blue (Duksan Pure Chemical Co.) were used as adsorbents. The physical properties of the adsorbents are presented in Table 2. Before the experiment, zeolite 13X and silica gel were regenerated for more than 12 h at 593 K and 423 K, respectively.

In the adsorption experiment, humid air with the desired relative humidity was generated by the self-made humidity controller. The liquid water was injected on the nitrogen flow through the solenoid valve, which was controlled by the *in situ* hygrometer (VAISARA, HMD40U). Also, the vapor-generating line was heated by a heating tape to protect the generated humid air from condensation and the feed flow rate was controlled by a precalibrated mass flow controller (Bronkhorst High-Tech, F-201C). The final feed temperature and relative humidity were measured by another hygrometer located in front of the bottom of the bed. The effluent gas was also monitored by both the hygrometer (VAISARA, HMD40U) and dew-point meter (Panametrics, MMS 35) located above the top of the bed.

In the regeneration experiment, the self-made tubular heater and the heating tape were used to produce the hot purge gas with the desired regeneration temperature. Two

Table 2. Physical Properties of Adsorbents

	Zeolite 13X	Silica Gel
Form	Bead	Bead
Partical size	4–8 mesh	4–8 mesh
BET surface area	402 m^2/g	716 m^2/g
Particle void fraction	0.24	0.28
Particle density	1.10 g/cm^3	1.22 g/cm^3
Heat capacity	1.1 J/g·K	0.92 J/g·K
Averaged isosteric heat of adsorption	62.7 kJ/mol	50.2 kJ/mol

J-type thermocouples were installed between the adsorption bed and the tubular heater to control the temperature of the purge gas. The flow rate of the hot purge gas was measured by both a rotameter (Dwyer, RMA-23-SSV) and a wet-gas meter (Shinagawa, W-NK-1B). The effluent was condensed by a heat exchanger, and the amount of the condensed liquid was measured in real time by the microbalance. All the experimental data, including temperature, pressure, feed flow rate, humidity, and mass in a microbalance were saved on a computer.

The adsorption bed was made of a stainless steel pipe with a length of 30 cm, 3.3 cm ID, and 0.23 mm wall thickness. While the feed mixture flowed upward in the adsorption bed in the adsorption breakthrough, the hot purge gas flowed downward along the bed in the regeneration breakthrough. Five J-type thermocouples were installed at positions 5, 10, 15, 20, and 25 cm from the bottom of the bed in order to measure the temperature in the bed. The bed was wrapped in glass wool. The pressure was measured at the top and bottom of the bed. The single adsorbent bed was packed with the zeolite 13X. In the layered bed, the silica gel and the zeolite 13X were packed in a volume ratio of 9 to 21. The silica gel was located in the lower part of the bed and the zeolite 13X was in the upper part of the bed. The characteristics of the adsorption bed are listed in Table 1.

Results and Discussion

Zeolite 13X bed vs. layered bed

While the equilibrium isotherm of water in the zeolite 13X was highly favorable, similar to that in zeolite 5A, in the experimental range of this study, the isotherm in the silica gel was close to a linear type (Yang, 1987; Ryu et al., 2001). The adsorption capacity of the silica gel for water was superior to that of the zeolite 13X, where the RH was higher than 55%. Therefore, in order to dry a feed gas of over 50% RH, it is expected that a layered bed with silica gel and zeolite 13X can show better performance than a single bed of zeolite 13X, because the silica gel layer treats a feed with high water concentration as a bulk separator, and then the zeolite 13X layer performs the purification of the pretreated humid air. In this study, the adsorption and regeneration characteristics in the zeolite 13X bed were compared with those in the layered bed (silica gel : zeolite 13X = 9 : 21 in volume ratio).

Figure 1 shows the adsorption breakthrough curve and the temperature excursion in the zeolite 13X bed under conditions of 9 LSTP/min feed flow rate, 12,740 ppm (54% RH at 293 K) feed concentration, and 295 K. The temperature inside the bed was steeply increased due to the high heat of adsorption. While the front part of the temperature profile propagated to the product end much faster than the concentration wavefront, the rear part of the temperature profile kept pace with the concentration wavefront. As a result, a broad temperature profile was formed at each position of the bed, as shown in Figure 1a. However, although a large temperature excursion occurred in the bed, the breakthrough curve in Figure 1b was relatively steep due to a strong self-sharpening effect.

In order to evaluate the performance of the layered bed, the adsorption breakthrough experiment in the layered bed was performed under conditions similar to that in the single

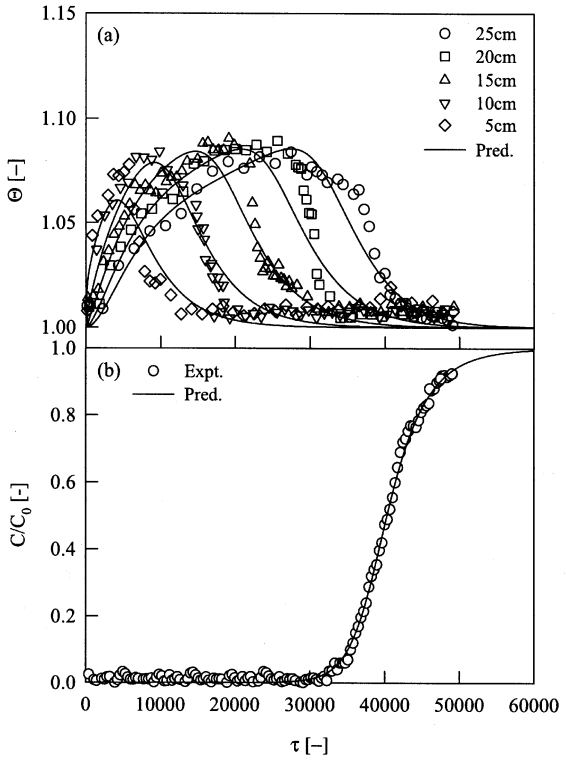

Figure 1. Experiment and simulation of the adsorption breakthrough in the zeolite 13X bed at 9 LSTP/min feed flow rate, 12,740 ppm (54% RH at 293 K), and 295 K ambient temperature.

(a) Dimensionless temperature profile, and (b) dimensionless effluent concentration.

bed. Figure 2 represents the adsorption breakthrough curve and the temperature excursion in the layered bed [silica gel (S): zeolite 13X (Z) = 9 : 21 in volume ratio] under the conditions of 9 LSTP/min feed flow rate, 12,800 ppm (49% RH at 295 K) feed concentration, and 296 K. In addition, the simulated results in the layered beds with different volume ratios of silica gel and zeolite 13X were compared with the zeolite 13X and silica gel beds under the same operation condition in Figure 2.

In Figure 2a, the overall temperature profiles in the layered bed (S:Z = 9:21) were more dispersive than that in the zeolite 13X bed. In addition, the maximum temperature excursion at each position of the layered bed was smaller than that in the zeolite 13X bed. In particular, the temperature excursion in the silica gel layer was much lower than that in the same position of the zeolite 13X bed due to the weak adsorption of water in the silica gel. However, as the feed passed through the zeolite 13X layer, this dispersive temperature wavefront formed in the silica gel layer became steeper and the temperature profile in the layered bed became similar to that in the zeolite 13X bed near the product end. This phenomenon could be explained by the adsorption breakthrough curves at various layered beds in Figure 2b.

In Figure 2b, the simulated result in the silica gel bed showed an early breakthrough time and a very broad breakthrough curve due to the relatively linear isotherm and slow

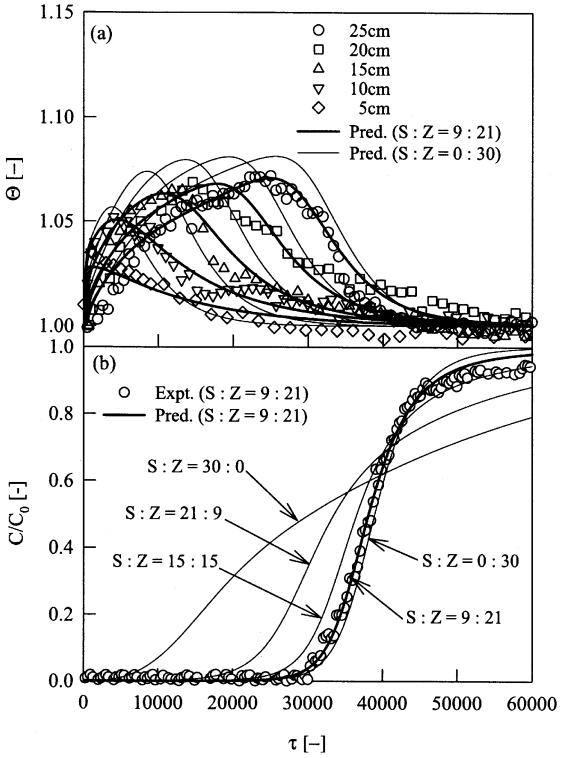

Figure 2. Experiment and simulation of the adsorption breakthrough in the layered bed (silica gel: zeolite 13X = 9 : 21) at 9 LSTP/min feed flow rate, 12,800 ppm (49% RH at 295 K), and 296 K ambient temperature.

(a) Dimensionless temperature profile, and (b) comparison of dimensionless effluent concentrations in the layered beds with various volume ratios of silica gel (S) and zeolite 13X (Z).

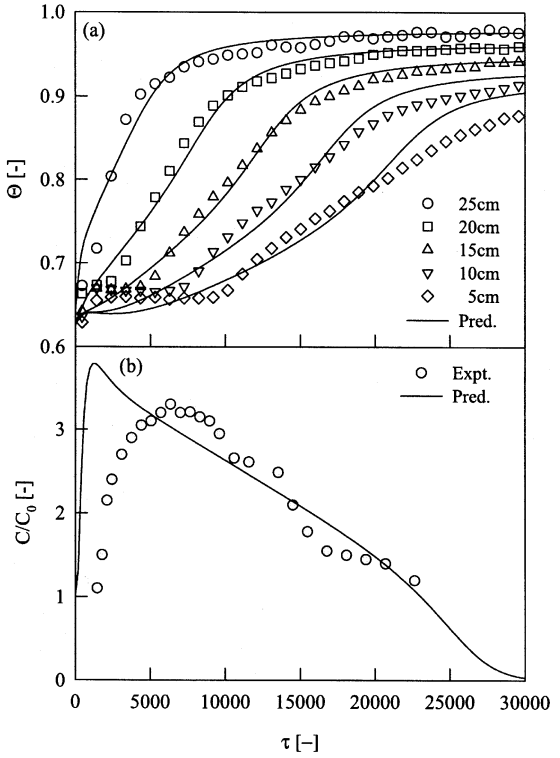

Figure 3. Experiment and simulation of the thermal regeneration breakthrough in the zeolite 13X bed at 26 LSTP/min feed flow rate, 473 K purge temperature, and 295 K ambient temperature.

(a) Dimensionless temperature profile, and (b) dimensionless effluent concentration. Adsorption condition: 12,740 ppm (54% RH at 293 K) and 295 K ambient temperature.

adsorption rate in silica gel even though the water adsorption capacity of silica gel was similar to that of zeolite 13X at the operation condition. Therefore, it was expected that the use of the silica gel bed would be very inefficient in the air-drying TSA process, because some part of the bed remained unused.

Because the zeolite 13X layer portion was greater, the breakthrough curve was steeper, and its shape became similar to that in the zeolite 13X bed, similar to the results of the temperature profiles at the product end in Figure 2b. In the case of the layered bed (S : Z = 9 : 21), the water breakthrough occurred slightly earlier in the layered bed than in the zeolite 13X bed in spite of similar adsorption capacity in both beds. In addition, the breakthrough curve in the layered bed showed a longer tailing than that in the zeolite 13X bed due to more dispersive MTZ in the layered bed. However, as can be seen in Figure 2b, the adsorption breakthrough differed little in both beds.

Figures 3 and 4 show the thermal regeneration breakthrough curves of the zeolite 13X bed and the layered bed (S : Z = 9 : 21) presaturated in the adsorption breakthrough experiments in Figures 1 and 2, respectively. In both cases, the regeneration condition was 26 LSTP/min purge flow rate, 473 K purge temperature, and 295 K ambient temperature. In the regeneration experiment, the desorbed water vapor was condensed into water drops by passing the heat exchanger in order to measure the amount of the desorbed water. Since the amount of the desorbed water was measured in the form of the continual water drops, the experimental data could be considered as a time-average value. As shown in Figures 3 and 4, the deviation between the experiment and the prediction in the regeneration breakthrough resulted from the time-average value in the microbalance. In particular, some deviation in the initial part of the regeneration curve was observed due to the condensation on the inner wall of the heat exchanger. Moreover, a small amount of the desorbed water vapor passed out of the heat exchanger without condensation under the saturation condition in the heat exchanger. Therefore, a certain amount of uncondensed water was added to the desorbed water measured in the microbalance.

Recently, Šťpánek et al. (2000) proposed a good isotherm model that could describe a hysteresis-dependent isotherm and applied to the air-drying PSA process under isothermal conditions. However, it was hard to adapt the isothermal process assumption in this study owing to the large temperature variation in Figures 1 to 4. And there are few articles for isotherm models including the hysteresis phenomena and temperature-dependency simultaneously. However, if the hysteresis phenomena of water on silica gel in the isotherm

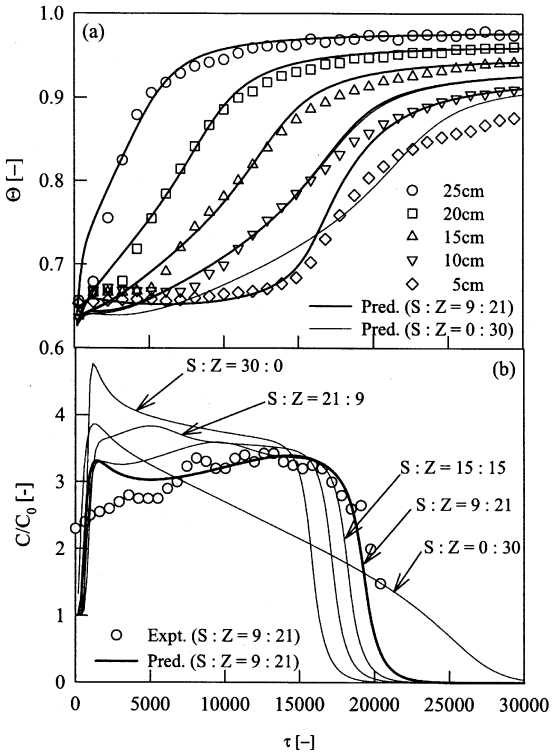

Figure 4. Experiment and simulation of the thermal regeneration breakthrough in the layered bed (silica gel : zeolite 13X = 9 : 21) at 26 LSTP/min feed flow rate, 473 K purge temperature, and 295 K ambient temperature.

(a) Dimensionless temperature profile, and (b) comparison of dimensionless effluent concentrations in the layered beds with various volume ratios of silica gel (S) and zeolite 13X (Z). Adsorption condition: 12,800 ppm (49% RH at 295 K) and 296 K ambient temperature.

model were applied to the simulation of the thermal regeneration breakthrough, the simulated amount of desorption in the initial part of the regeneration curve will be smaller than the present result in Figure 4.

In Figure 3a, the temperature at the lower part of the bed was not changed for a certain period of time due to the large heat capacity of water and the high heat of desorption. Therefore, during this initial period of regeneration breakthrough, the water vapor thermally desorbed in the upper part of the bed was readsorbed in the lower part of the bed.

Since water on zeolite 13X showed strong favorable adsorption and the adsorption amount was less sensitive to temperature variation, the adsorbed water could not be desorbed easily by increasing the bed temperature. Therefore, it took a long time to regenerate the bed completely by heating the bed, as shown in Figure 3b. Furthermore, the bed temperature at 5 cm from the bottom of the bed in Figure 3a could not approach the steady-state until the regeneration was completely finished.

The most salient difference between the temperature profiles of the layered bed (S : Z = 9 : 21) and the zeolite 13X bed was observed in the bed temperature at 5 cm from the bottom of the bed. In Figure 4a, the temperature increase at the silica gel layer in the layered bed was slower than that at the same position in the zeolite 13X bed. However, after passing some period of regeneration time, the temperature at the silica gel layer in the layered bed increased much faster than that at the zeolite layer in the zeolite 13X bed.

Because the amount of water adsorption on silica gel drastically decreased with an increase in temperature, the silica gel bed could be more effectively regenerated than the zeolite 13X bed by hot gas. As shown in Figure 4b, as the part of the bed packed with silica gel was larger, the time required to regenerate the bed became shorter. In particular, the complete regeneration time could be drastically reduced compared to that in the zeolite 13X bed if the lower part of the zeolite 13X bed was packed with silica gel. However, enlargement of a portion of the silica gel layer could not lead to the drastic decrease of the complete regeneration time. As a result, the layered bed with a narrow silica gel layer was recommended in the air-drying TSA because the layered bed with a large portion of silica gel showed a bad performance in the adsorption breakthrough in Figure 2b.

As shown in Figure 4b, at the initial regeneration breakthrough, the amount of the desorbed water was smaller in the layered bed (S : Z = 9 : 21) than in the zeolite 13X bed due to greater readsorption in the silica gel layer. However, when there is an increase in bed temperature, the silica gel is regenerated more easily than zeolite 13X. Therefore, as the thermal wavefront approached the lower part of the bed, the amount of the desorbed water became greater in the layered bed in Figure 4a than that in the zeolite 13X bed in Figure 4b. After showing a desorption plateau in the layered bed, the slope of the concentration wavefront became much steeper than that in the zeolite 13X due to weak affinity of water in the silica gel.

In sum, silica gel should be placed in the lower part of the fixed bed in the air-drying TSA process, because the desorption dynamics of the lower part of the bed was more important in determining the time required to regenerate the bed completely than that of the upper part of the bed.

Zeolite 13X bed vs. layered bed TSA processes

Basmadjian (1975) suggested that a thermal wavefront, called "pure thermal wave," could precede a concentration wavefront if his proposed criteria were satisfied. In this case, the dynamics of adsorption breakthrough was independent of the initial bed temperature.

Water adsorption and desorption in this study were apt to satisfy the criteria for the existence of a pure thermal wave because of its relatively low concentration in the feed stream and its high equilibrium loading. The criterion ratio, R, was in the range of 17–455 for various drying processes in use (Basmadjian, 1975). Since the criterion ratio, R, in this study was around 21, there was a rational reason for the omission of the cooling step in designing the air-drying TSA process.

Based on the dynamic study, the two-bed air-drying TSA process was simulated under nonadiabatic and adiabatic conditions. The cycle of the TSA process was composed of adsorption and regeneration steps without a cooling step in which each step time was 4 h. The feed stream flowed upward in the adsorption step, and the purge stream flowed downward in the regeneration step. The adsorption bed in

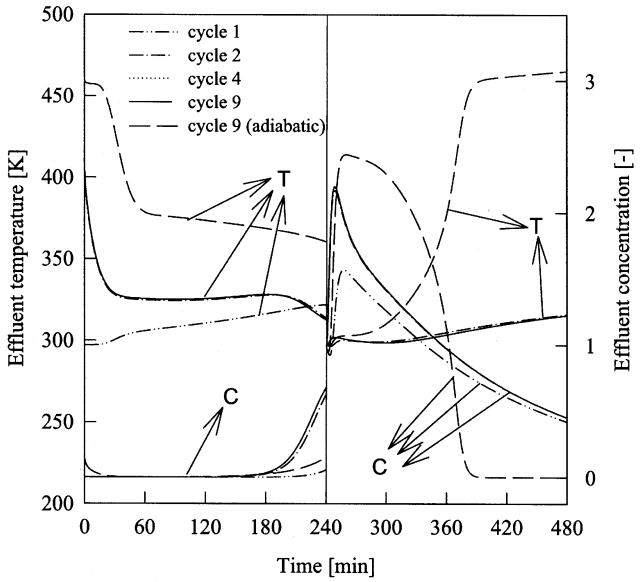

Figure 5. Simulation of the TSA process of zeolite 13X bed with adsorption step (4 h) and thermal regeneration step (4 h) under the adiabatic and nonadiabatic conditions.

Adsorption condition: 17,800 ppm, 9 LSTP/min feed rate, 297 K ambient temperature. Regeneration condition: 11 LSTP/min, 483 K purge temperature, 297 K ambient temperature.

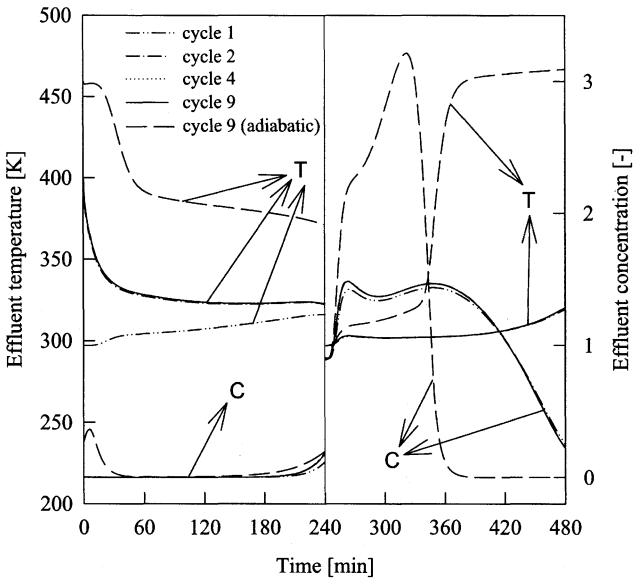

Figure 6. Simulation of the TSA process of layered bed (silica gel : zeolite 13X = 9:21) with adsorption step (4 h) and thermal regeneration step (4 h) under the adiabatic and nonadiabatic conditions.

Adsorption condition: 17,800 ppm, 9 LSTP/min feed rate, 297 K ambient temperature. Regeneration condition: 11 LSTP/min, 483 K purge temperature, 297 K ambient temperature.

the TSA process was the same size as the one used in breakthrough experiment.

In the case of the simulation of the TSA process in the zeolite 13X bed, the adsorption and regeneration dynamics approached the cyclic steady state within the fourth cycle, as shown in Figure 5. Compared with the regeneration breakthrough at 26 LSTP/min purge flow rate in Figure 3, the effluent temperature under the nonadiabatic condition increased little at 11 LSTP/min purge flow rate. Therefore, the effluent concentration at the end of the regeneration step at 11 LSTP/min purge flow rate was around 0.45 of the feed concentration. Consequently, under this operating condition, the adsorption bed was not completely regenerated within the regeneration step time given in the simulation. This incomplete regeneration led to the discharge of a small amount of water, around 0.68 of the feed concentration at the end of the adsorption step.

However, in the adiabatic condition, the effluent temperature increased steeply to the desired regeneration temperature during the regeneration step. After the completion of regeneration, the effluent temperature approached the hot purge temperature very slowly. Moreover, a small amount of water was discharged at the product stream in the initial period of the adsorption step due to the high bed temperature in the adiabatic condition. However, since the adsorption bed was completely regenerated in the regeneration step time, the effluent concentration in the adiabatic condition did not increase as much as in the nonadiabatic condition at the end of the adsorption step.

Figure 6 represents the cyclic performance of the TSA process in the layered bed with the silica gel and zeolite 13X in a volume ratio of 9 : 21, respectively. The cyclic process approached the cyclic steady state within the fourth cycle, which was the same as in the zeolite 13X bed. Under the nonadiabatic condition, the effluent concentration at the end of the regeneration step was around 0.22 in the layered bed, which was less than half of the effluent concentration in the zeolite 13X bed in Figure 5. The adsorption bed could be regenerated more efficiently in the layered bed at 11-LSTP/min purge flow rate than in the zeolite 13X bed. As a result, at the end of the adsorption step, the effluent concentration of water was around 0.18 of the feed concentration in the layered bed, which was significantly lower than in the zeolite 13X bed.

Similar to the regeneration dynamics in the layered bed in Figure 4b, the initial regeneration in the layered bed at the nonadiabatic condition was worse than in the zeolite 13X bed, because the water desorbed in the upper bed was readsorbed in the silica gel layer more than in the zeolite 13X layer. However, as the thermal wavefront approached the lower part of the bed, a larger amount of water was discharged in the layered bed than in the zeolite 13X bed, because the equilibrium adsorption amount of water in the silica gel layer had more sensitive dependence on temperature than that in the zeolite 13X layer. Under the adiabatic condition, the effluent temperature in the layered bed approached the temperature of the hot purge gas faster than that in the zeolite 13X bed. This was because complete regeneration could be accomplished within a shorter time in the layered bed than that in the zeolite 13X bed. As a result, the air-drying TSA process can be operated more efficiently in the layered bed than in the zeolite 13X bed. Moreover, since the commercial air-dry-

ing TSA processes are generally operated under adiabatic conditions, the layered-bed TSA process can save more energy in view of the regeneration time and temperature than the zeolite 13X bed TSA process.

Conclusions

The dynamics of the adsorption and thermal regeneration breakthrough of water in a fixed bed were studied to understand the adsorption dynamic behavior of the air-drying TSA process. A proper nonequilibrium mathematical model that considers nonisothermal and nonadiabatic conditions was developed. Since the flange effect was similar to the heat transfer by extended surface equipment, it was included in this mathematical model as an additional boundary condition at the adsorption and regeneration steps.

The adsorption and thermal regeneration characteristics in the single bed with zeolite 13X were compared with those in the layered bed (silica gel : zeolite 13X = 9 : 21 in volume ratio). Although the layered bed had a similar adsorption capacity as the zeolite 13X bed under this experimental condition, it showed slightly earlier water breakthrough and longer tailing in the adsorption breakthrough due to the dispersive concentration wavefront in the silica gel layer. However, the regeneration characteristics of the layered bed were significantly enhanced in comparison to those of the zeolite 13X bed because of the weak adsorption of water in the silica gel layer.

In designing the air-drying TSA process, the cooling step could be omitted according to the Basmadjian's criterion for pure thermal wave. In the layered-bed TSA process, the regeneration of the adsorption bed was more efficiently performed than in the zeolite 13X bed TSA process. As a result, the effluent concentration of water at the end of the adsorption step was significantly lower in the layered bed than in the zeolite 13X bed.

Acknowledgment

The financial support of the Korea Research Foundation (KRF-2001-005-E0031) is gratefully acknowledged. This article was presented at the 7th International Conference on Fundamentals of Adsorption, Nagasaki, Japan, in May 2001.

Notation

A = dimensionless group; or area, cm^2
A' = dimensionless group
$B \backsim H$ = dimensionless group
b = Langmuir–Freudlich model parameter, kPa^{-1}
c = concentration, mol/cm^3
c_i = concentration of component i, mol/cm^3
C_p = heat capacity, $J/g \cdot K$
D_L = axial dispersion, cm^2/s
h = heat-transfer coefficient, $J/cm^2 \cdot s \cdot K$
L = length of adsorption bed, cm
K_L = effective axial thermal conductivity, $J/cm \cdot s \cdot K$
k = overall mass-transfer coefficient in LDF model, s^{-1}
n = Langmuir–Freundlich model parameter
P = pressure, kPa
P_i = partial pressure of component i, kPa
Pe_m = Peclet number in mass transfer
Pe_h = Peclet number in heat transfer
q = adsorbed phase concentration, mol/g
q_m = Langmuir–Freudlich model parameter, mol/g
$\bar{q}$ = volume-averaged adsorbed-phase concentration, mol/g
Q = dimensionless adsorbed-phase concentration
Q_m = dimensionless Langmuir–Freudlich model parameter
$\bar{Q}$ = dimensionless volume-averaged adsorbed-phase concentration
R = radius, cm; or gas constant, $J/mol \cdot K$
t = time, s; or thickness, cm
t_F = axial length of flange, cm
T = temperature, K
u = interstitial velocity, cm/s
y = mass fraction of a component
z = axial distance along adsorption bed, cm
$\triangle H$ = isosteric heat of adsorption, J/mol

Greek letters

α = total void fraction
ϵ = bed void fraction
ζ = dimensionless axial distance along the bed
η = fin efficiency
Θ = dimensionless temperature
τ = dimensionless time
ρ = density, g/cm^3

Superscript and subscripts

$*$ = equilibrium state
0 = constant value
a = adsorbed phase
atm = atmospheric
B = bed
c = concentration
f = feed
F = flange
g = gas phase
i = inner
o = outer
p = pellet or plateau
s = solid phase
tot = total
w = wall

Literature Cited

Ahn, H., C.-H. Lee, B. Seo, J. Yang, and K. Baek, "Backfill Cycle of a Layered Bed H_2 PSA Process," *Adsorption,* **5**, 419 (1999).
Ahn, H., *Adsorption and Thermal Regeneration of Water in a Fixed-Bed of Air-Drying TSA Process,* PhD Diss., Yonsei Univ., (2002).
Basmadjian, D., "On the Possibility of Omitting the Cooling Step in Thermal Gas Adsorption Cycles," *Can. J. Chem. Eng.,* **53**, 234 (1975).
Basmadjian, D., K. D. Ha, and C.-Y. Pan, "Nonisothermal Desorption by Gas Purge of Single Solutes in Fixed-Bed Adsorbers. I. Equilibrium Theory," *Ind. Eng. Chem. Process Des. Dev.,* **14**, 328 (1975).
Carter, J. W., and H. Husain, "The Simultaneous Adsorption of Carbon Dioxide and Water Vapor by Fixed Beds of Molecular Sieves," *Chem. Eng. Sci.,* **29**, 267 (1974).
Davis, M. M., and M. D. LeVan, "Equilibrium Theory for Complete Adiabatic Adsorption Cycles," *AIChE J.,* **33**(3), 470 (1987).
Farooq, S., and D. M. Ruthven, "Heat Effect in Adsorption Column Dynamics. 1. Comparison of One- and Two Dimensional Models," *Ind. Eng. Chem. Res.,* **29**, 1076 (1990).
Huang, C.-C., and J. R. Fair, "Study of the Adsorption and Desorption of Multiple Adsorbateds in a Fixed Bed," *AIChE J.,* **34**, 1861 (1988).
Hwang, K.-S., D.-K. Choi, S.-Y. Gong, and S.-Y. Cho, "Adsorption and Thermal Regeneration of Methylene Chloride Vapor on an Activated Carbon Bed," *Chem. Eng. Sci.,* **52**, 1111 (1997).
Kumar, R., and G. R. Dissinger, "Nonequilibrium, Nonisothermal Desorption of Single Adsorbate by Purge," *Ind. Eng. Chem. Process Des. Dev.*, **25**, 456 (1986).

Lee, C.-H., J. Yang, and H. Ahn, "Effects of Carbon-to-Zeolite Ratio on Layered Bed H_2 PSA for Coke Oven Gas," *AIChE J.,* **45**, 535 (1999).

Liu, Y., and J. A. Ritter, "Evaluation of Model Approximations in Simulating Pressure Swing Adsorption-Solvent Vapor Recovery," *Ind. Eng. Chem. Res.,* **36**, 1767 (1997).

Park, J.-H., J.-N. Kim, S.-H. Cho, J.-D. Kim, and R. T. Yang, "Adsorber Dynamics and Optimal Design of Layered Beds for Multicomponent Gas Adsorption," *Chem. Eng. Sci.,* **53**(23), 3951 (1998).

Rege, S. U., R. T. Yang, Q. Kangyi, and M. A. Buzanowski, "Air-Prepurification by Pressure Swing Adsorption Using Single/Layered Beds," *Chem. Eng. Sci.,* **56**, 2745 (2001).

Reid, R. C., J. M. Prausnitz, and B. E. Poling, *The Properties of Gases and Liquids,* McGraw-Hill, Singapore (1988).

Ruthven, D. M., S. Farooq, and K. S. Knaebel, *Pressure Swing Adsorption,* VCH Publishers, New York (1994).

Ryu, Y. K., S. J. Lee, J. W. Kim, and C.-H. Lee, "Adsorption Equilibrium and Kinetics of H_2O on Zeolite 13X," *Korean J. Chem. Eng.,* **18**, 525 (2001).

Schork, J. M., and J. R. Fair, "Parametric Analysis of Thermal Regeneration of Adsorption Beds," *Ind. Eng. Chem. Res.,* **27**, 457 (1988).

Št Pánek, F., M. Kubíček, M. Marek, M. Šoóš, P. Rajniak, and R. T. Yang, "On the Modeling of PSA Cycles with Hysteresis-Dependent Isotherms," *Chem. Eng. Sci.,* **55**, 431 (2000).

Watson, C. F., R. D. Whitley, and M. L. Meyer, "Multiple Zeolite Adsorbent Layers in Oxygen Separation," U.S. Patent No. 5,529,610 (1996).

Yang, J., and C.-H. Lee, "Adsorption Dynamics of a Layered Bed PSA for H_2 Recovery from Coke Oven Gas," *AIChE J.,* **44**, 1325 (1998).

Yang, R. T., *Gas Separation by Adsorption Processes,* Butterworths, Boston, MA (1987).

Manuscript received Sept. 2, 2002, and revision received Jan. 6, 2003.